

Percolation and Magnetization for Generalized Continuous Spin Models

Santo Fortunato and Helmut Satz

Fakultät für Physik, Universität Bielefeld
D-33501 Bielefeld, Germany

Abstract:

For the Ising model, the spin magnetization transition is equivalent to the percolation transition of Fortuin-Kasteleyn clusters; this result remains valid also for the conventional continuous spin Ising model. The investigation of more general continuous spin models may help to obtain a percolation formulation for the critical behaviour in $SU(2)$ gauge theory. We therefore study a broad class of theories, introducing spin distribution functions, longer range interactions and self-interaction terms. The thermal behaviour of each model turns out to be in the Ising universality class. The corresponding percolation formulations are then obtained by extending the Fortuin-Kasteleyn cluster definition; in several cases they illustrate recent rigorous results.

Introduction

Percolation theory [1, 2] has been successfully applied to describe continuous thermal phase transitions as geometrical transitions: at the critical threshold, suitably defined clusters become infinite (see [3] - [6]). It is moreover possible to establish a correspondence between thermal and cluster variables, such that the critical exponents of corresponding variables coincide [4]. This provides an intuitive geometric description of the mechanism of the thermal transition; e.g., in the case of the Ising model, we can identify clusters as magnetic domains, so that magnetization sets in when they span the lattice. In a recent study [7], we have tried to extend this picture to the confinement-deconfinement transition of $SU(2)$ gauge theory. This theory leads to a continuous phase transition which belongs to the universality class of the Ising model, due to the common $Z(2)$ global symmetry of the corresponding Hamiltonians [8]. However, our result is valid only in the strong coupling limit of $SU(2)$, where the partition function can be well approximated [9] by that of a continuous spin Ising model. In this model, the correspondence between percolation and thermal variables can be rigorously established [10, 11]. For a general study of $SU(2)$ gauge theory, the weak coupling limit must be taken into account, and there the approximations used in [9] are no longer valid.

To address the deconfinement problem more generally, it may be helpful to look for an effective theory for $SU(2)$. An interesting attempt in this direction was proposed some time ago in the search for the fixed point of the theory by means of block-spin transformations [12]. There the original Polyakov loop configurations were projected onto configurations of Ising-like spins according to the sign of the Polyakov loop at each lattice

site. This assumes that for the criticality only the global $Z(2)$ symmetry of the theory is important. As a result of this projection one obtains an effective Hamiltonian with only short-range couplings, although some of the resulting couplings correspond to interactions beyond the fundamental nearest-neighbour form. Moreover, the assumption that only the $Z(2)$ symmetry of the theory is relevant must be tested.

In this work we investigate several spin models in order to get a better understanding of the behaviour of the $SU(2)$ effective theory. Our investigations are based on lattice Monte Carlo simulations of the various models.

We focus on continuous spin Ising models, in which the individual spins s_i at each lattice site can take on all values in the finite range $[-1, 1]$, with the distribution of the spins governed by a spin distribution function $f(s_i)$. For $f(s_i) = \delta(|s_i| - 1) \forall i$ and only nearest-neighbour (NN) interactions, we recover the conventional Ising model. For $f(s_i) = 1 \forall i$ and only NN interactions, we obtain the continuous spin model studied in [10]. Here we will consider four more general models of this type (d denotes the space dimension):

- A) $d = 2$, only NN interactions, but a non-uniform spin distribution $f(s_i)$;
- B) $d = 2$, $f(s_i) = 1 \forall i$, NN and diagonal next-nearest-neighbour (NTN) interaction (Fig. 1);
- C) $d = 3$, $f(s_i) = 1 \forall i$, NN and two types of NTN interactions (see Fig. 2);
- D) as case C), but including an additional self-interaction term proportional to $s_i^2 \forall i$.

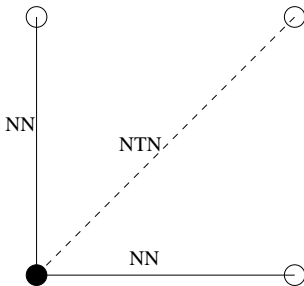


Figure 1. Spin interactions in model B.

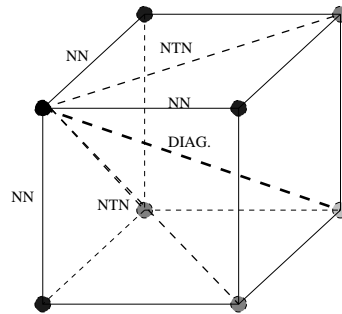


Figure 2. Spin interactions in model C.

We will first present a detailed numerical investigation of the thermal critical behaviour and show that each model belongs to the same universality class as the Ising model. Subsequently, we provide a suitable cluster definition in order to interpret the thermal phase transition of the models as a geometrical percolation transition. Concerning the second issue, it was recently proven rigorously that the result of [10] can be extended to the models A, B and C [11]. We believe, however, that it is useful to illustrate it by exploiting the power of the finite-size scaling analysis. On the other hand, model D has

not been investigated so far; as self-interactions play an important role in gauge theories, it is interesting to examine what happens in this case.

Model A: Spin Distribution Function

The spin variable s can take all values in $[-1, 1]$. It is convenient to rewrite it in the form

$$s = \text{sign}(s)\sigma, \quad (1)$$

separating the sign from the amplitude of the spin. Since we want to retain the $Z(2)$ symmetry of the Hamiltonian, the signs of the spins are equidistributed. In contrast, the amplitudes can in general be weighted in different ways by choosing a distribution function $f(\sigma)$. The partition function of such a model then has the form

$$Z(T) = \prod_i \int_0^1 d\sigma_i f(\sigma_i) \exp\{\kappa \sum_{\langle i,j \rangle} s_i s_j\}, \quad (2)$$

where $\kappa \equiv J/T$, with J denoting the spin coupling energy and T the temperature. Since we want to study models with continuous transitions, the choice of the function $f(\sigma)$ is not arbitrary. It can be proved that it must obey certain regularity conditions, which are not very restrictive, however [13]. In [10], the amplitudes were equidistributed, with $f(\sigma) = 1$. Here we consider the following form for $f(\sigma)$:

$$f(\sigma) = \sqrt{1 - \sigma^2} \quad (3)$$

which is the Haar measure of the $SU(2)$ group; it appears in the strong coupling approximation of $SU(2)$ [9]. To define a cluster, we use exactly the same procedure as in [10], i.e., we join nearest-neighbouring spins of the same sign with the bond probability $p = 1 - \exp(-2\kappa\sigma_i\sigma_j)$, where σ_i and σ_j are the amplitudes of the two spins. We use free boundary conditions and define percolation when a cluster spans the lattice in each of the two directions. This is done to exclude the possibility that, due to the finite size of our lattices, one could find more than one percolation cluster, which would make the definition of our variables ambiguous. We shall use this definition for all the models to be considered here¹.

The percolation variables to be studied are: the *percolation strength* P ,

$$P = \frac{\text{size of the percolating cluster}}{\text{volume of the lattice}}. \quad (4)$$

and the *average cluster size* S ,

$$S = \frac{\sum_s n_s s^2}{\sum_s n_s s}. \quad (5)$$

Here n_s is the number of clusters of size s and the sums exclude the percolating cluster. Besides these two, we evaluate another very useful variable. For a given lattice size and a value of κ , we determine the relative fraction of configurations containing a percolating

¹In three dimensions even this definition of a spanning cluster does not exclude the possibility of having more than one such cluster in the same configuration. Nevertheless the occurrence of these cases is so small that we can safely ignore them.

cluster. This variable, that we shall call *percolation cumulant* and indicate as $\gamma_r(\kappa)$, is a scaling function, analogous to the Binder cumulant $g_r(\kappa)$ [14].

In addition to these percolation variables, we also measure the lattice averages of energy and magnetization, in order to study the thermal transition as well. From the magnetization M we calculate in particular the physical susceptibility χ ,

$$\chi(\kappa) = V (\langle M^2 \rangle - \langle M \rangle^2) \quad (6)$$

and the Binder cumulant g_r ,

$$g_r(\kappa) = \frac{\langle M^4 \rangle}{\langle M^2 \rangle^2}. \quad (7)$$

We have performed simulations on four lattice sizes, from 64^2 to 240^2 . Our algorithm consists in heatbath steps for the update of the spin amplitudes followed by Wolff-like cluster updates for the flipping of the signs. That is basically the same method as used in [10], although the heatbath procedure is slightly modified to take into account the presence of the distribution function $f(\sigma)$. The proof that the detailed balance condition is satisfied for such a cluster update is obtained following the derivations in [15] - [18]. Flipping the spins reduces drastically the autocorrelation time, which allowed us to collect extensive data and thus reduce the errors.

Fig. 3 shows a comparison between the thermal variable $g_r(\kappa)$ and the percolation cumulant $\gamma_r(\kappa)$, both as functions of the temperature variable κ , for different lattice sizes. The points where the lines cross are the infinite volume thresholds for the thermal and the geometrical transition, respectively. The agreement between the two points is remarkable.

Since the percolation cumulant is a scaling function, we can already get an indication about the critical exponents of the percolation transition. Given the critical point and the exponent ν , a rescaling of the percolation cumulant as a function of $(\kappa - \kappa_{cr})L^{1/\nu}$ should give us the same function for each lattice size (L is the linear dimension of the lattice). Figs. 4 and 5 show the rescaled percolation cumulant, using $\kappa_{cr} = 1.3888$ with the random percolation exponent $\nu = 4/3$ and Ising exponent $\nu = 1$, respectively. The figures clearly show scaling for the Ising exponent and no scaling for the random percolation exponent.

The exponent β governs percolation strength and magnetization, while γ governs cluster size and susceptibility. To determine them, we have performed high-statistics simulations around the critical point, with the number of measurements for each value of the coupling varying from 50000 to 100000. We have then used the χ^2 method [19] to determine the values of the exponents. The results are shown in Table I, where the first row shows the calculated percolation results, the second the corresponding magnetization calculations, and the third the analytically known Ising model values. It is evident that the percolation behaviour coincides fully with the thermal critical behaviour. This conclusion holds in general for all admissible distribution functions, as it was shown in [11].

Model B: Next-to-Nearest Neighbour Interactions

We now want to study how to correctly define clusters in the presence of more than the standard nearest-neighbour interactions. We have now two terms, with a Hamiltonian

of the form

$$\mathcal{H} = -J_{NN} \sum_{\langle i,j \rangle}^{NN} s_i s_j - J_{NTN} \sum_{\langle i,j \rangle}^{NTN} s_i s_j \quad (8)$$

where the first sum describes nearest-neighbour and the second diagonal next-to-nearest neighbour interactions (Fig. 1). Since longer range interactions are generally weaker, we fix the ratio between the two couplings at $J_{NN}/J_{NTN} = 10$; however, we do not believe that our results depend on the choice of the couplings, as long as both are ferromagnetic. To define clusters, we now extend the Coniglio-Klein method and define for each two spins i, j of the same sign, for NN as well as NTN, a bond probability

$$p_B^x = 1 - \exp\{-2\kappa_x \sigma_i \sigma_j\}, \quad (9)$$

where x specifies $\kappa_{NN} = J_{NN}/T$ and $\kappa_{NTN} = J_{NTN}/T$, respectively. We recall that in model B, as well as in C and D, we assume a spin equidistribution, i.e., $f(\sigma) = 1$.

We have studied model B using two different Monte Carlo algorithms, in order to test if a Wolff-type algorithm can also be applied in the presence of NTN interactions. The first is the standard Metropolis update, while the second alternates heat bath steps and a generalized Wolff flipping, for which the clusters are formed taking into account both interactions. The generalization of the cluster update is trivial. After several runs, some with high statistics, we found excellent agreement with the Metropolis results in all cases. So, the mixed algorithm with heat bath and Wolff flippings appears to remain viable also in the presence of more than the standard NN interaction. Subsequently we have therefore used this mixed algorithm. The lattice sizes for model B ranged from 100^2 to 400^2 .

As for model A, we now show for model B the comparison between percolation cumulant and Binder cumulant, in order to test that the critical points coincide (Fig. 6). We then again rescale the percolation cumulant, using the critical κ determined in Fig. 6 together with the exponent ν from the $d = 2$ random percolation transition ($\nu = 4/3$) and the $d = 2$ Ising model ($\nu = 1$). Figs. 7 and 8 indicate that again the correct exponent is that of the Ising model.

The determination of the other two exponents β and γ by means of the χ^2 method confirms that indeed both the thermal and the geometrical exponents belong to the Ising universality class (Table II).

Model C: Extension to Three Dimensions

We have here repeated the study for a $d = 3$ model with three different interactions (Fig. 2). To fix the model, we have to specify the ratios of the nearest-neighbour coupling κ_{NN} to κ_{NTN} and κ_{diag} . We chose them to be 10:2 and 10:1, respectively. Our $d = 3$ calculations are performed on lattices ranging from 12^3 to 40^3 .

Also here we have first compared the results from a mixed algorithm of the same kind as for the previous case to those from a standard Metropolis algorithm; again, the agreement is very good. Figs. 9, 10 and 11 then show the comparison of the thresholds and the scaling of the percolation cumulant. As before, the correspondence between percolation and thermal variables is evident (Table III).

Model D: Adding Self-Interaction

From what we have seen up to now, it seems to be clear that the correct cluster definition can readily be extended to models including several (ferromagnetic) spin-spin interactions. However, such terms are not the only possible interactions in a model with $Z(2)$ symmetry and a continuous transition. There could be anti-ferromagnetic spin-spin couplings as well as multispin terms, coupling an even number of spins greater than two (four, six, etc.). Moreover, since the spins are continuous, the presence of self-interaction terms is possible, determined by s^2 , s^4 , etc. The treatment for antiferromagnetic and multispin couplings so far remains an open question. In contrast, self-interactions are not expected to play a role in the cluster building, since such terms do not relate different spins. Therefore, we test a cluster definition ignoring any self-interaction term.

We thus consider in Model D the same interactions as in Model C, plus a term proportional to $J_0 \sum_i s_i^2$. We chose a negative value for the self-interaction coupling J_0 ; this is the more interesting case since the corresponding interaction tries to resist the approach of the system to the ground state at low temperatures ($\sigma = 1$ everywhere). The ratios of the NN coupling to the others were chosen as $J_{NN} : J_{NTN} : J_{diag} : |J_0| = 6 : 2 : 1 : 2$.

Again we first verify the viability of the mixed algorithm and then determine the rescaled percolation cumulant (Fig. 12) and the critical exponents (Table IV). It is evident that the percolation and the thermal transition again fall into the Ising universality class.

Conclusions

We have performed a complete investigation of several continuous spin models, obtained from the simple model studied in [10] by introducing a distribution function for the spin amplitudes, longer-ranged interactions and self-interactions. The thermal behaviour leads in all cases to the Ising universality class. All systems admit equivalent percolation formulations; for models A, B and C, we illustrate numerically the analytical results found in [11]. All the features of the models we studied are expected to enter in the further extension to $SU(2)$ gauge theories, and the fact that they do not interfere with a percolation formulation of critical behaviour provides support for such efforts.

Acknowledgements

It is a pleasure to thank D. Gandolfo for helpful discussions. We would also like to thank the TMR network ERBFMRX-CT-970122 and the DFG Forschergruppe Ka 1198/4-1 for financial support.

References

- [1] D. Stauffer, A. Aharony, *Introduction to Percolation Theory*, Taylor & Francis, London 1994.
- [2] G. Grimmett, *Percolation*, Springer-Verlag, 1999.
- [3] M. E. Fisher, *Physics* **3**, 255-283 (1967).

- [4] A. Coniglio, W. Klein, J. Phys. A. **13**, 2775 (1980).
- [5] L. Chayes, Comm. Math. Phys. **197**, 623 (1998).
- [6] M. Campbell, L. Chayes, J. Phys. A. **31**, L255-L259 (1998).
- [7] S. Fortunato, H. Satz, Phys. Lett. B **475**, 311-314 (2000).
- [8] B. Svetitsky, L. G. Yaffe, Nucl. Phys. B **210**, 423 (1982).
- [9] F. Green, F. Karsch, Nucl. Phys. B **238**, 297 (1984).
- [10] P. Bialas et al, hep-lat/9911020, Nucl. Phys. B (in press).
- [11] P. Blanchard, L. Chayes, D. Gandolfo, Nucl. Phys. B **588**, 229 (2000).
- [12] M. Okawa, Phys. Rev. Lett. **60**, 1805-1808 (1988).
- [13] R. S. Ellis, J. L. Monroe, C. M. Newman, Comm. Math. Phys. **46**, 167-182 (1976).
- [14] K. Binder, D. W. Heermann, *Monte Carlo simulations in Statistical Physics*, Springer-Verlag 1988.
- [15] U. Wolff, Nucl. Phys. B **322**, 759 (1989).
- [16] T. E. Harris, Proc. Camb. Phil. Soc. **56**, 13 (1960).
- [17] L. Chayes, J. Machta, Physica A **329**, 542 (1997).
- [18] L. Chayes, J. Machta, Physica A **254**, 477 (1998).
- [19] J. Engels et al., Phys. Lett. B **365**, 219 (1996).
- [20] A. M. Ferrenberg, D. P. Landau, Phys. Rev. B **44**, 5081 (1991).

	κ_{cr}	β/ν	γ/ν	ν
Percolation	$1.3887^{+0.0002}_{-0.0001}$	$0.128^{+0.007}_{-0.010}$	$1.754^{+0.007}_{-0.008}$	$0.99^{+0.03}_{-0.02}$
Magnetization	$1.3888^{+0.0002}_{-0.0003}$	$0.121^{+0.008}_{-0.006}$	$1.745^{+0.011}_{-0.007}$	$1.01^{+0.02}_{-0.03}$
Ising Model		1/8	7/4	1

Table I. Thermal and percolation thresholds and exponents of Model A.

	κ_{cr}	β/ν	γ/ν	ν
Percolation	$0.9708^{+0.0002}_{-0.0002}$	$0.129^{+0.008}_{-0.009}$	$1.752^{+0.009}_{-0.011}$	$1.005^{+0.012}_{-0.020}$
Magnetization	$0.9707^{+0.0003}_{-0.0002}$	$0.124^{+0.007}_{-0.005}$	$1.747^{+0.009}_{-0.007}$	$0.993^{+0.014}_{-0.010}$
Ising Model		1/8	7/4	1

Table II. Thermal and percolation thresholds and exponents of Model B.

	κ_{cr}	β/ν	γ/ν	ν
Percolation	$0.36673^{+0.00012}_{-0.00010}$	$0.528^{+0.012}_{-0.015}$	$1.9850^{+0.010}_{-0.015}$	$0.632^{+0.01}_{-0.015}$
Magnetization	$0.36677^{+0.00010}_{-0.00008}$	$0.530^{+0.012}_{-0.018}$	$1.943^{+0.019}_{-0.008}$	$0.640^{+0.012}_{-0.018}$
Ising Model [20]		$0.518^{+0.007}_{-0.007}$	$1.970^{+0.011}_{-0.011}$	$0.6289^{+0.0008}_{-0.0008}$

Table III. Thermal and percolation thresholds and exponents of Model C.

	κ_{cr}	β/ν	γ/ν	ν
Percolation	$0.3005^{+0.0001}_{-0.0001}$	$0.524^{+0.010}_{-0.011}$	$1.9750^{+0.008}_{-0.009}$	$0.636^{+0.011}_{-0.017}$
Magnetization	$0.3004^{+0.0002}_{-0.0001}$	$0.513^{+0.012}_{-0.010}$	$1.963^{+0.014}_{-0.009}$	$0.626^{+0.011}_{-0.010}$
Ising Model [20]		$0.518^{+0.007}_{-0.007}$	$1.970^{+0.011}_{-0.011}$	$0.6289^{+0.0008}_{-0.0008}$

Table IV. Thermal and percolation thresholds and exponents of Model D.

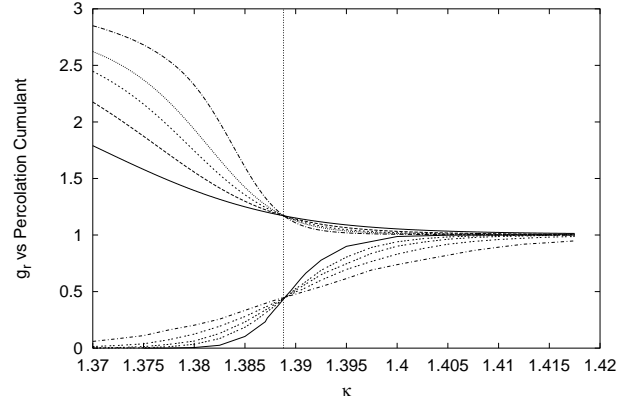


Figure 3. Comparison of the thermal and the geometrical critical point for Model A obtained respectively from the Binder cumulant g_r and the percolation cumulant.

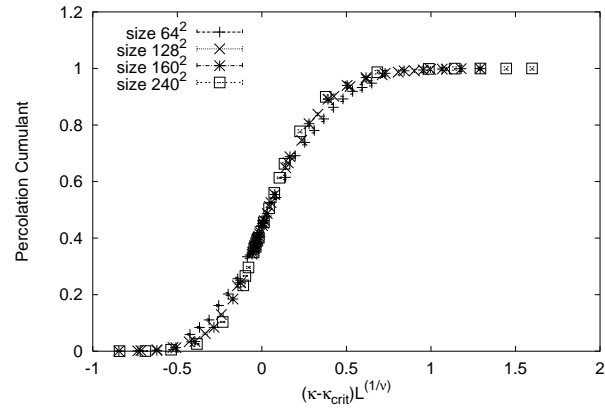


Figure 4. Rescaled percolation cumulants for Model A using the 2-dimensional random percolation exponent $\nu = 4/3$.

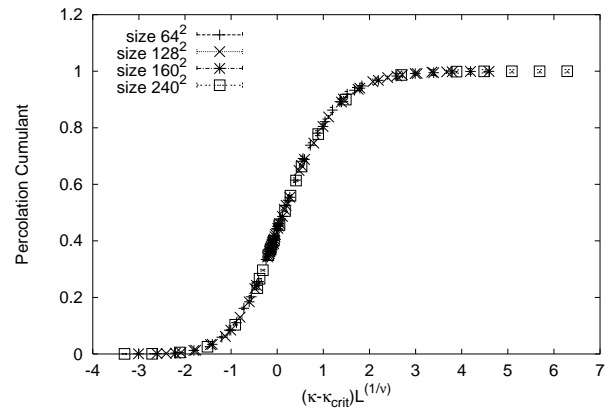


Figure 5. Rescaled percolation cumulants for Model A using the 2-dimensional Ising exponent $\nu = 1$.

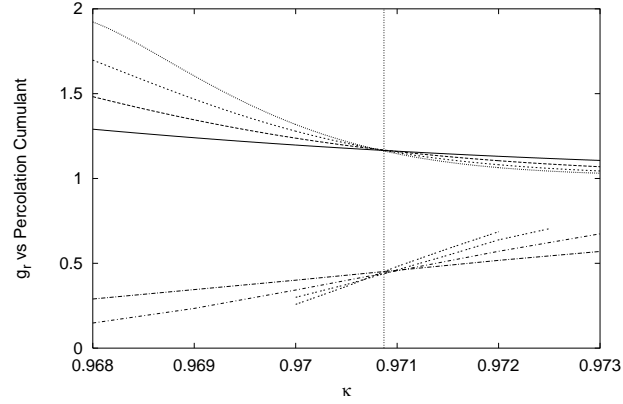


Figure 6. Comparison of the thermal and the geometrical critical point for Model B obtained respectively from the Binder cumulant g_r and the percolation cumulant.

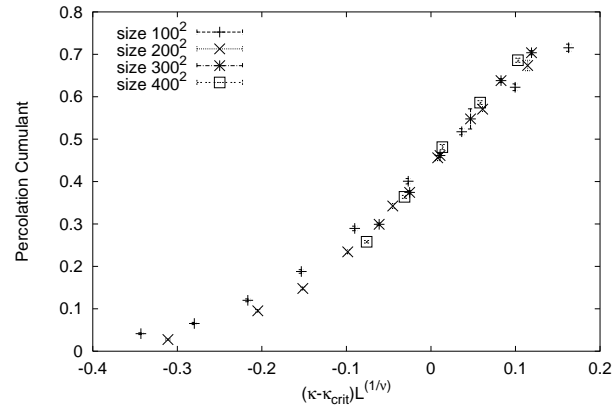


Figure 7. Rescaled percolation cumulants for Model B using the 2-dimensional random percolation exponent $\nu = 4/3$.

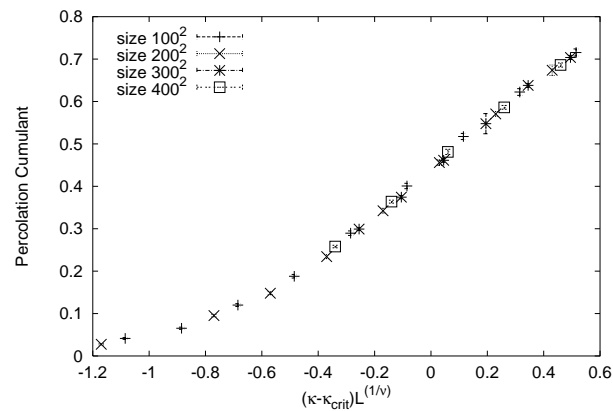


Figure 8. Rescaled percolation cumulants for Model B using the 2-dimensional Ising exponent $\nu = 1$.

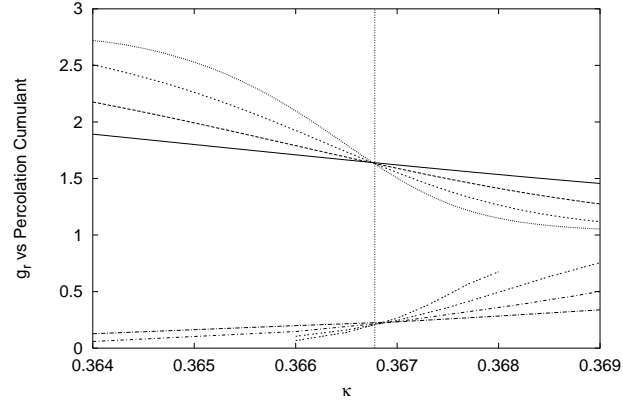


Figure 9. Comparison of the thermal and the geometrical critical point for Model C obtained respectively from the Binder cumulant g_r and the percolation cumulant.

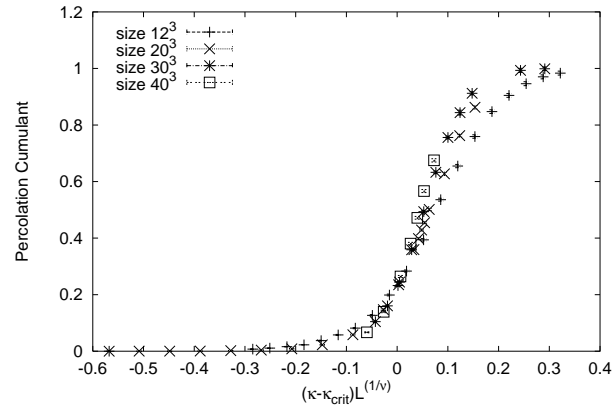


Figure 10. Rescaled percolation cumulants for Model C using the 3-dimensional random percolation exponent $\nu = 0.88$.

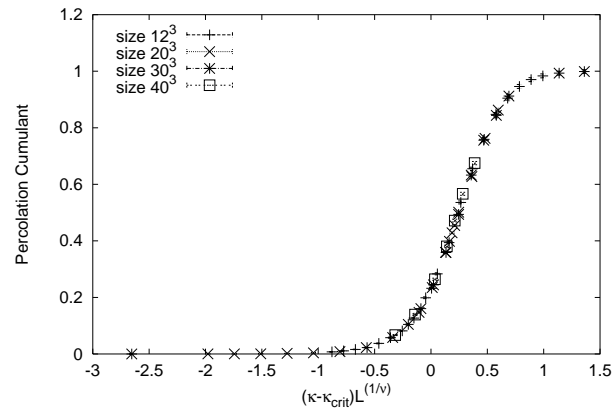


Figure 11. Rescaled percolation cumulants for Model C using the 3-dimensional Ising exponent $\nu = 0.6289$.

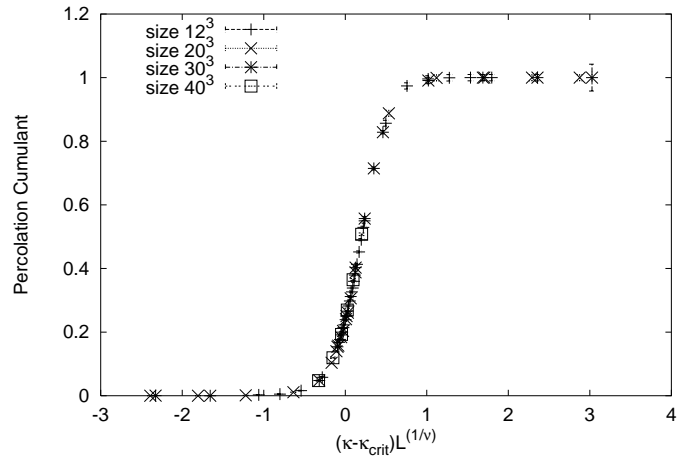


Figure 12. Rescaled percolation cumulants for Model D using the 3-dimensional Ising exponent $\nu = 0.6289$.

